Deutscher Wetterdienst
Wetter und Klima aus einer Hand

DWD

High Resolution Modelling of the Boundary Layer over the complex Terrain

Understanding thermally driven flow dynamics and weather forecasting in the Alps

Daniela Littmann[1], Alberto De Lozar[1], Chiara Marsigli[1,2], and Linda Schlemmer[1]

[1] Deutscher Wetterdienst (DWD), Offenbach am Main, Germany
[2] Arpae Emilia-Romagna, Bologna, Italy

1 October 2024

GL😊RI
GLObal to Regional ICON Digital Twin

June 2024: Storms over Central Europe

Figure: Hail (left) and flooding (right) in southern Germany.
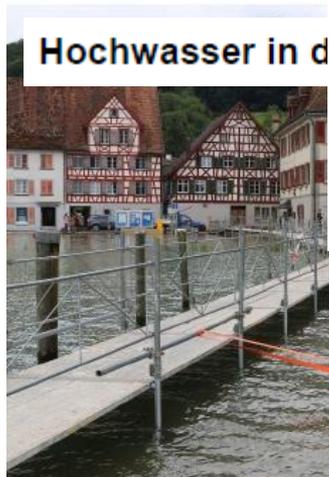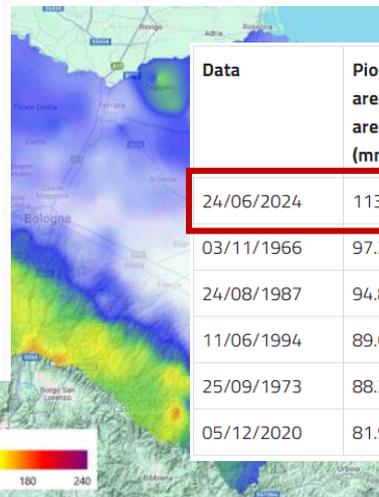Credit: ©Gewitterjäger, https://x.com/Gewitterjaeger/status/1799099655051178272.

Figure: Flooding (9-11 June) (Untersee) in Berlingen.
Credit: © D. Gerstgrasser, MeteoSchweiz 2024: Klimabulletin Juni 2024. Zürich.

Data	Pioggia media areale in 24h su area di allerta E (mm)
24/06/2024	113.7
03/11/1966	97.3
24/08/1987	94.8
11/06/1994	89.6
25/09/1973	88.3
05/12/2020	81.9

precipitation from 23 June, 2 m. in the Emilia-Romagna region. sured value of precipitation in mm during 24 hours.
Credit: © Arpae, https://www.arpae.it/, last access: 19.7.24.

The GLORI Digital Twin
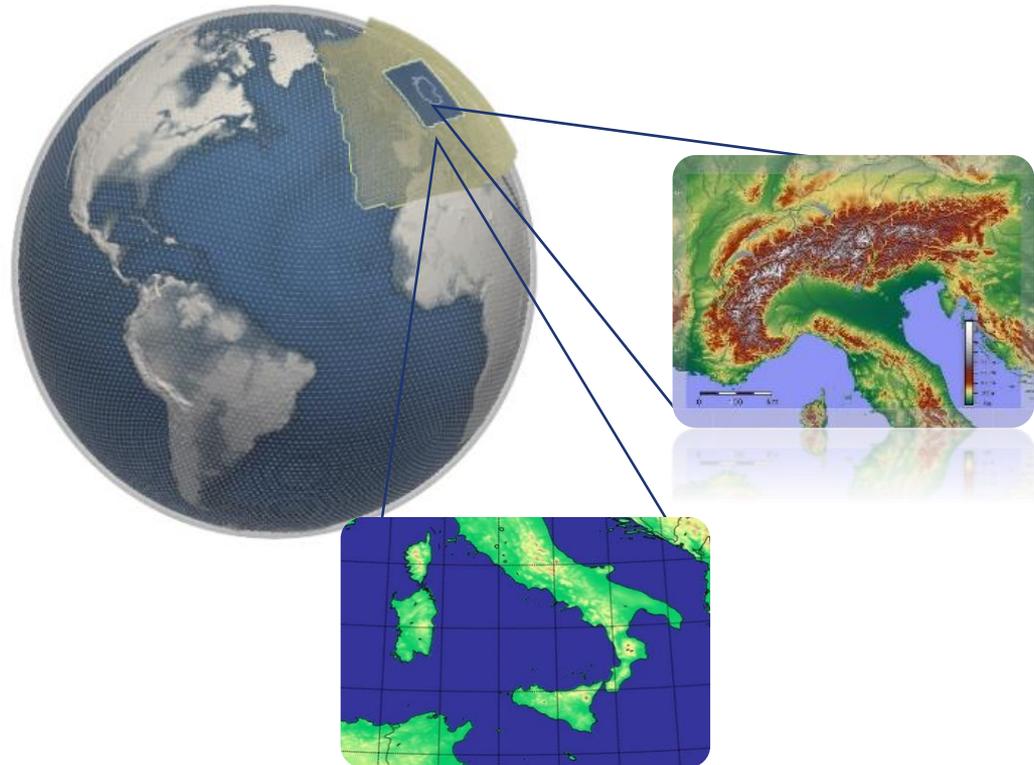
- Tri-lateral Cooperation Germany, Italy, Switzerland

- Global storm-resolving simulations (~ 3km) and regional high-resolved mesoscale simulations (500m)

- Extreme event prediction:
  → (Urban) Flooding
  → Pollen
  → Mineral Dust
  → (Urban) Heat Island

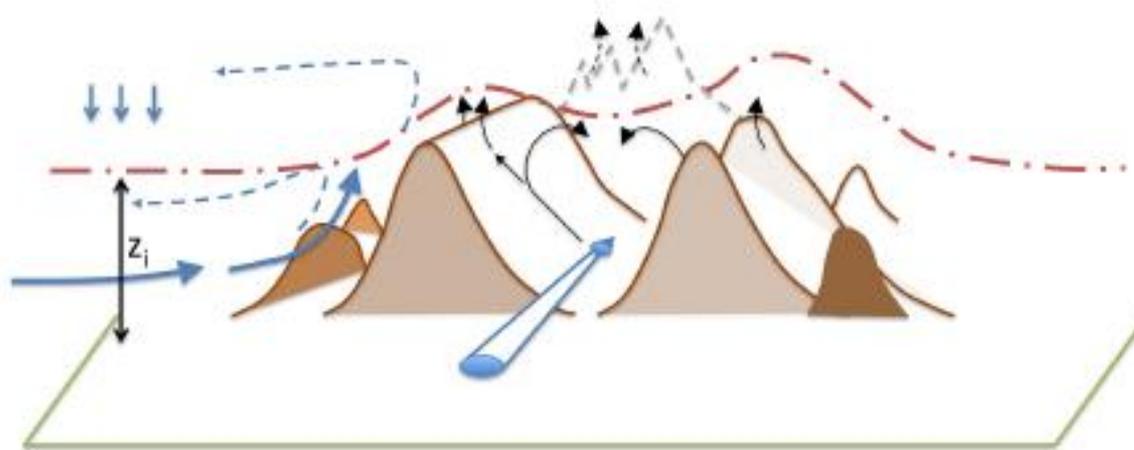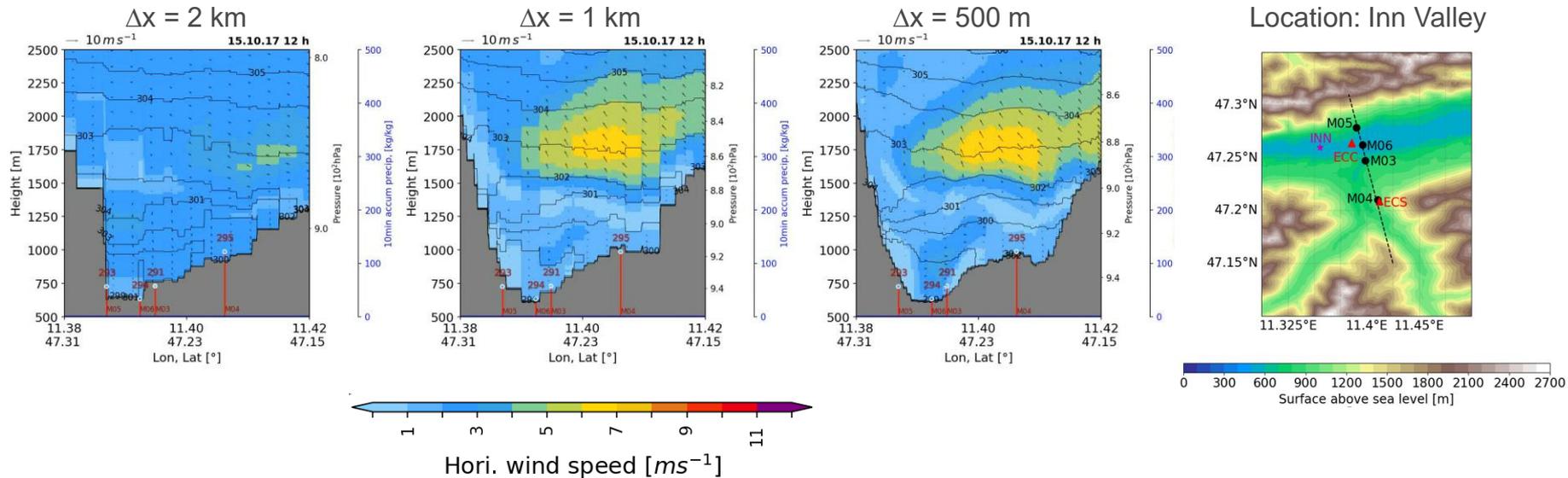# Thermal circulation in the Valley

<u>Figure:</u> Circulation pattern over the complex mountainous terrain during daytime.

z_i mixed layer height

⟶ plain-to mountain circulation & valley winds

⟶ slope-flow and venting

(Rotach et al. 2015)

Example: The Cold Air Pool 2017

Figures: Vertical cross sections in the Inn Valley (dashed line in right figure) for horizontal grid scales of 2 km, 1 km, and 500 m (left to right). Contours represent the averaged horizontal wind speed, arrows indicate the wind direction, contour lines show the potential temperature for a cold air pool case during the night of 15.-16. October 2017. Measurements from *Gohm et al. 2017* are marked as dots (right) and as lines (left). **A strong jet is resolved by higher resolutions → Impact on weather prediction?**

Model Domain

|	
Model top	22 km
Vertical level	65 full (66 half)
Hor. grid scale	2km, 1km, 500m
LATBC (at start)	Forecast (ICON-EU)
Forecast restart	12 h
Duration	36 h
1-way-Nesting	
Model version icon-2024.07	

Surface above sea level [m]
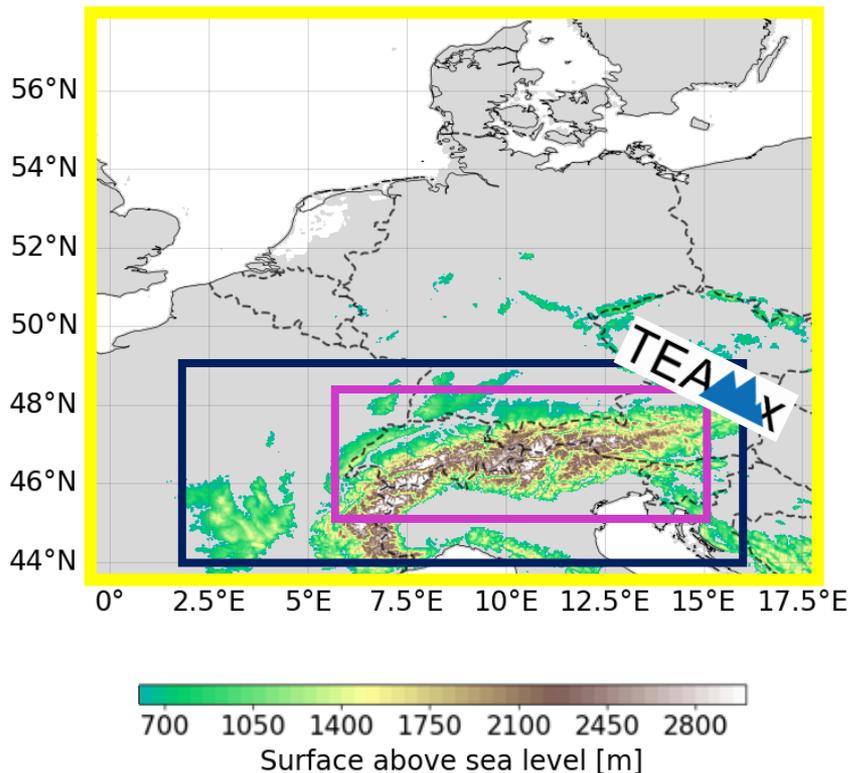
TEA▲▲x
Multi-scale Transport and
Exchange Processes in the
Atmosphere over
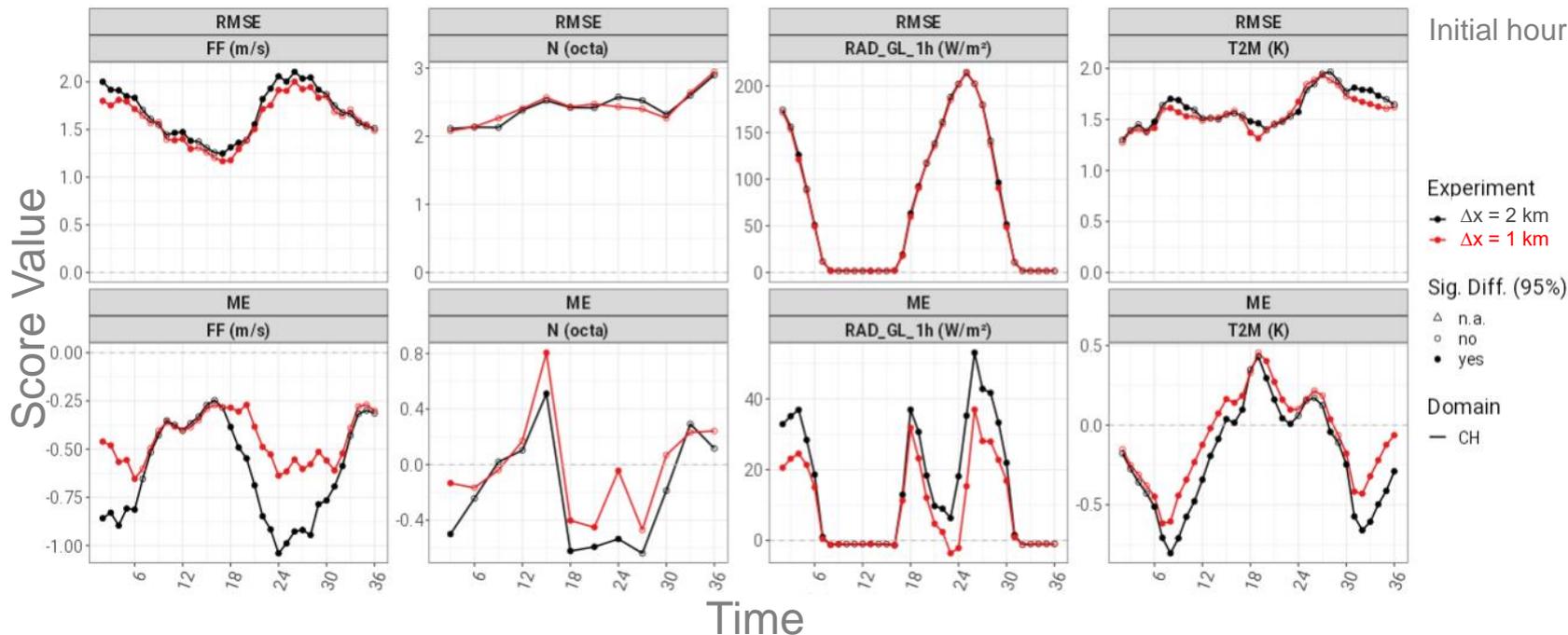Mountains –
Programme and experiment

Δx
2 km
1 km
500 m

GL❂RI
GLObal to Regional ICON Digital Twin
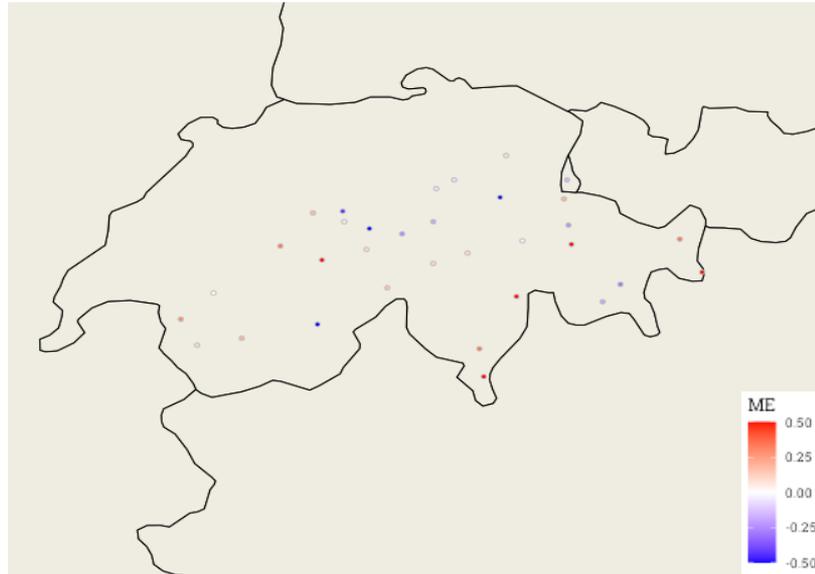
Valley Stations

Station	Wind speed	Temperature
Valley	25	34

<u>Figure:</u> The Valley stations used for the comparison to the model results. The colors show the mean error (ME) of the model for the temperature at 2m height above ground.
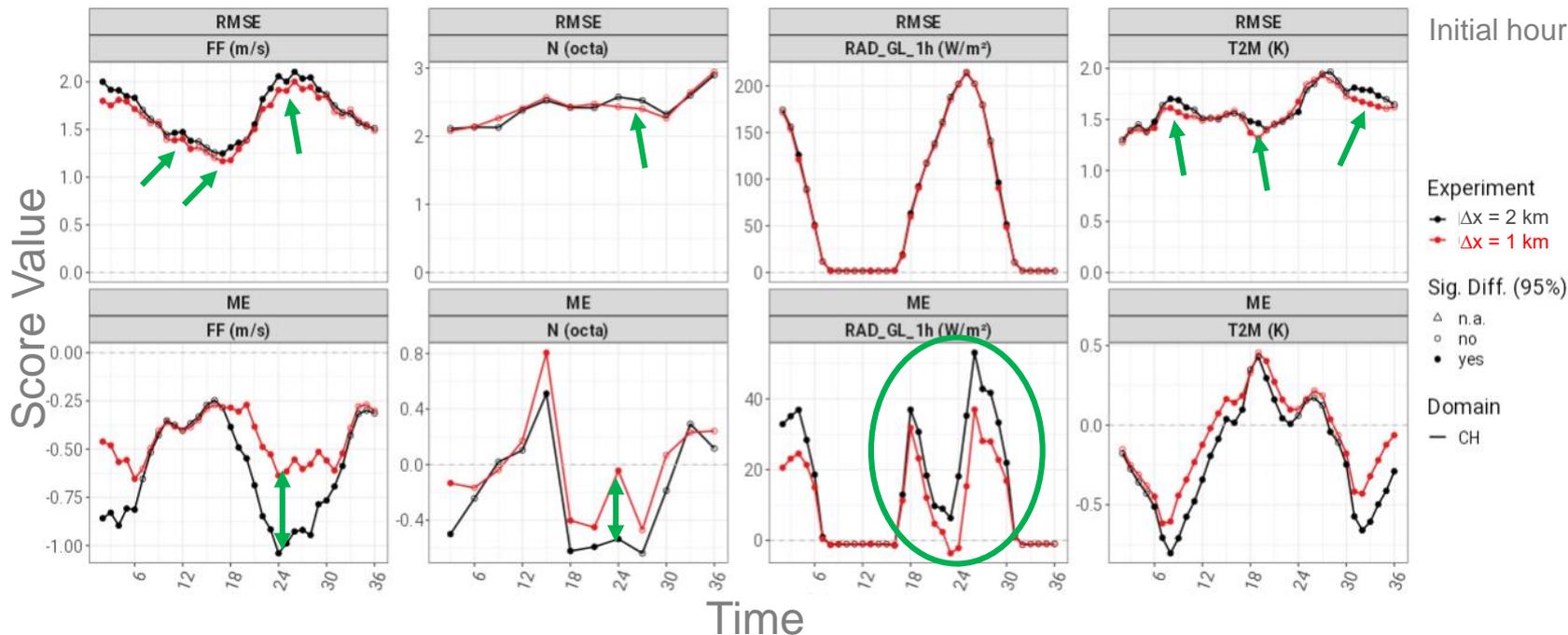
GL RI
GLObal to Regional ICON Digital Twin

RMSE (top) and ME (below) for May 2022

Valley Stations

RMSE (top) and ME (below) for May 2022

Initial hour: 12 h

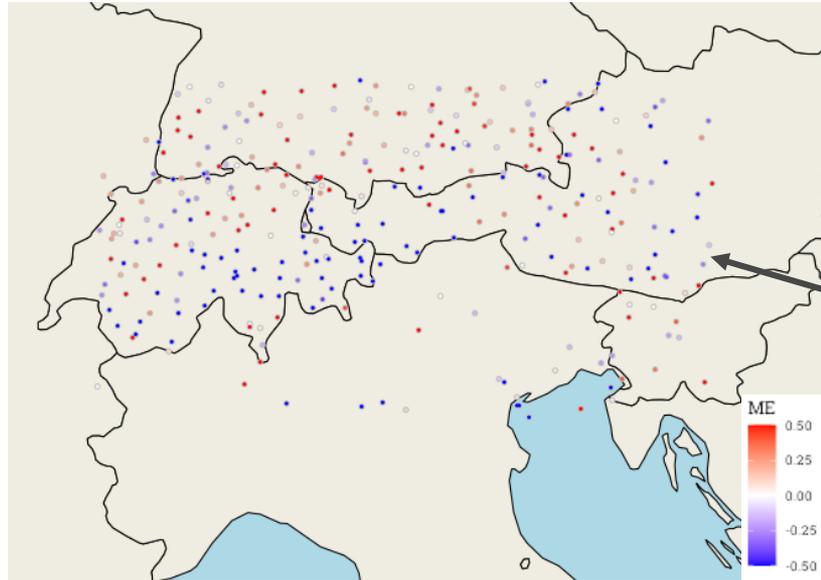- Improvement with increasing horizontal grid scale
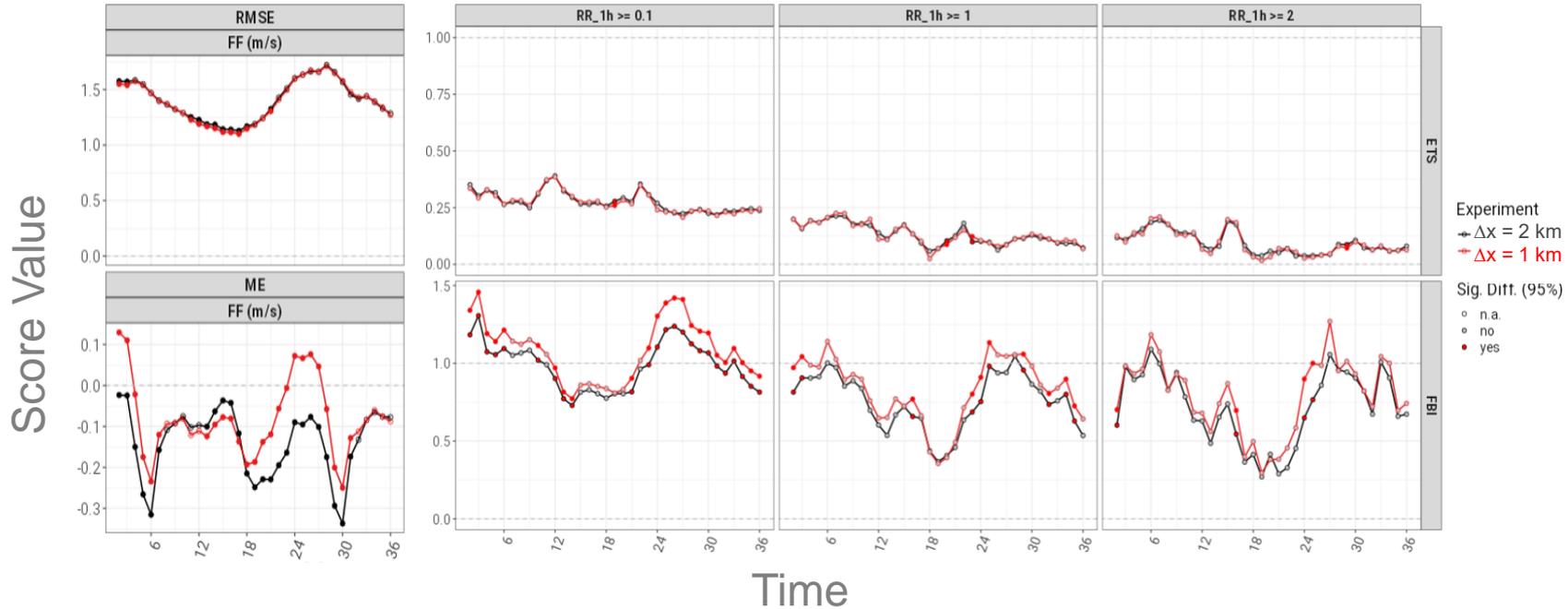
Observation

Figure: Meteorological stations used for the comparison to the model results. The colors of the dots show the mean error (ME) of the model for the temperature at 2m height above ground.
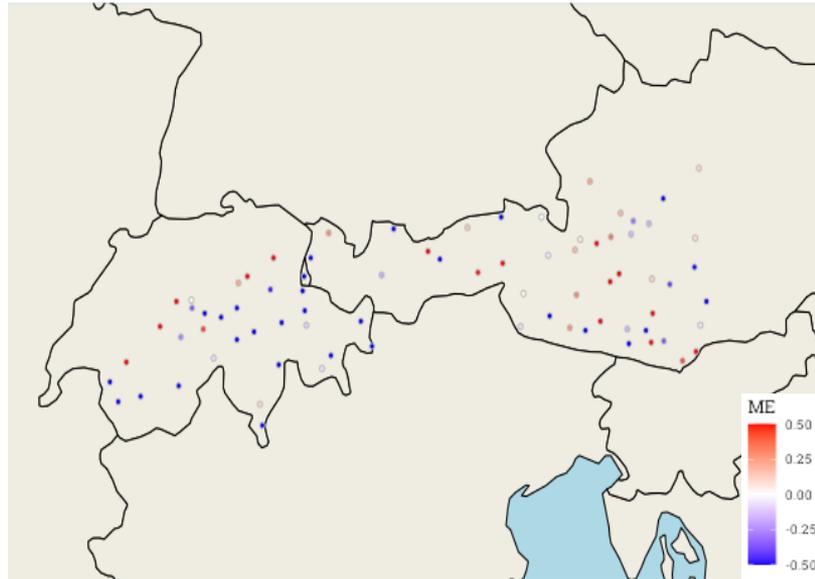
Only meteorological stations from the innermost TEAMx domain (ICON-A05) used for comparison.

- No clear benefit for weather prediction.
- As 1 km resolution is within grey zone → increase hori. grid scale, switch off parametrisations
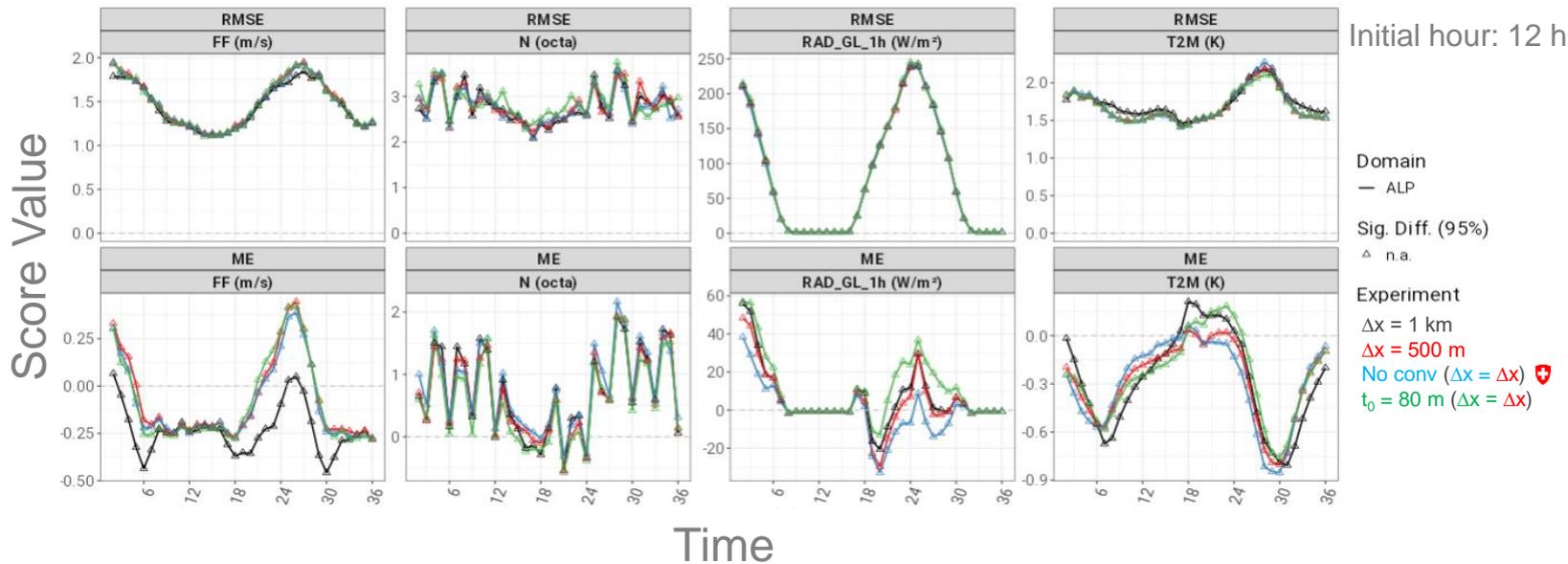
Valley Stations

Station	Wind speed	Temperature
Valley	73	79

Figure: The Valley stations used for the comparison to the model results. The colors show the mean error (ME) of the model for the temperature at 2m height above ground.
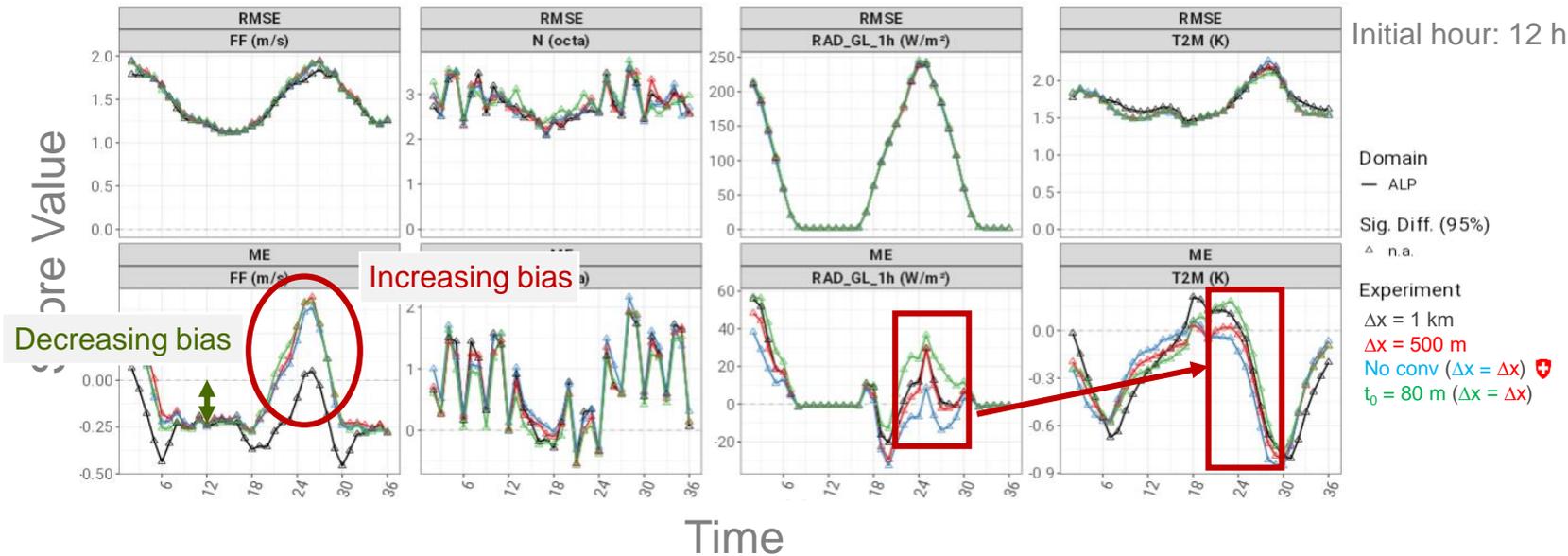
Valley Stations

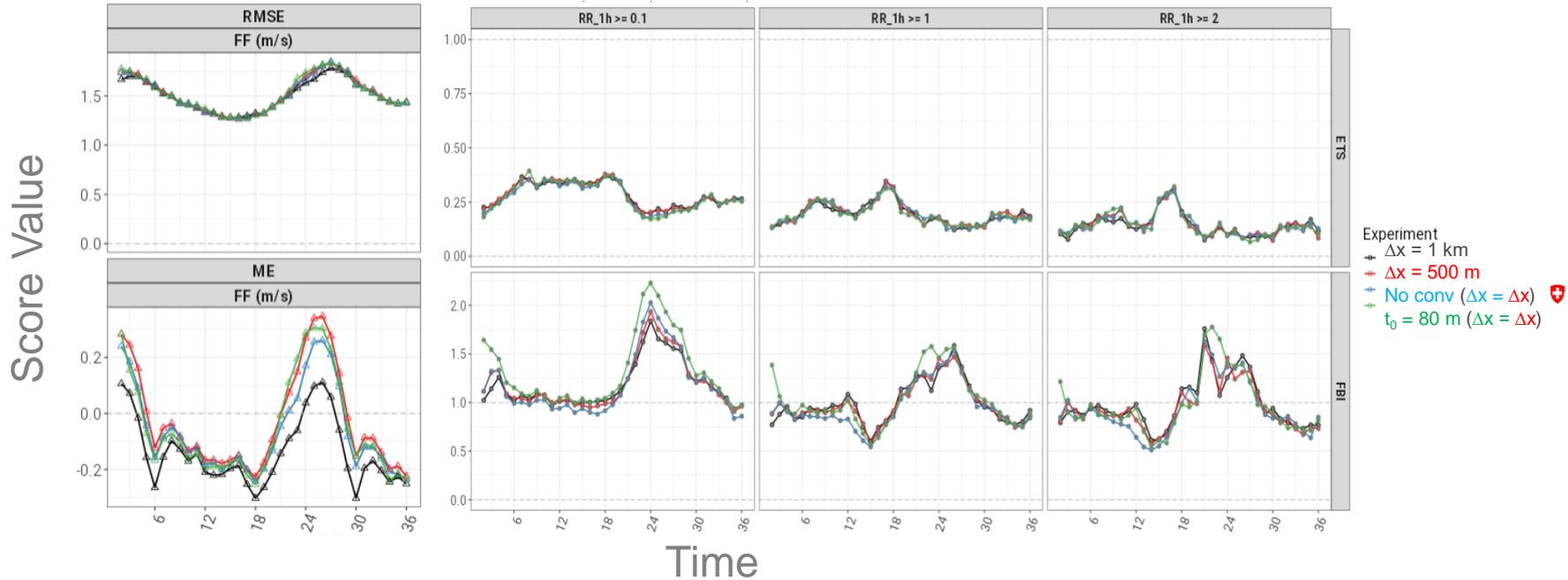RMSE (top) and ME (below) for June 2024

RMSE (top) and ME (below) for June 2024

- **Increasing bias** for wind speed during the day
- Comparative performance with switching off the convection scheme
- Besides total cloud cover, the drastic reduction of the TKE length scale does not improve
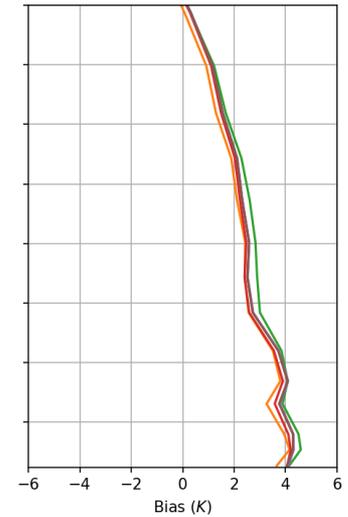
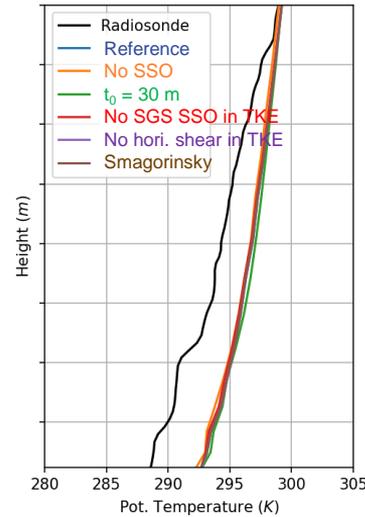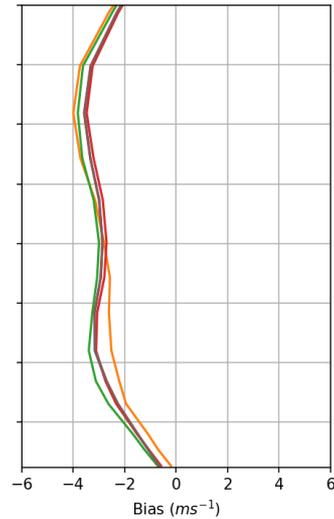- Modest changes for precipitation
- Do changes in the TKE play a minor role at these scales?

Turbulence in Case Study at Δx = 1km

Legend:
- Radiosonde
- Reference
- No SSO
- t_0 = 30 m
- No SGS SSO in TKE
- No hori. shear in TKE
- Smagorinsky

Turbulence in Case Study at Δx = 500m

16.10.2017 – 2 UTC
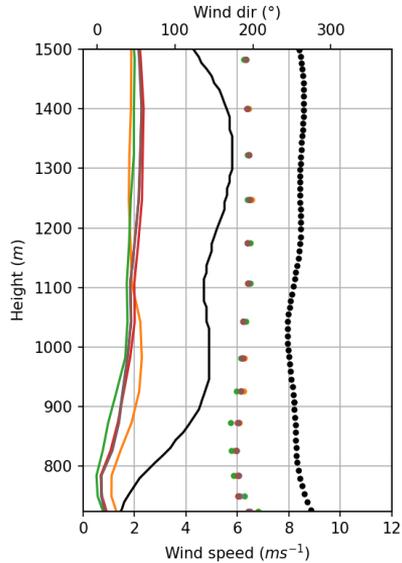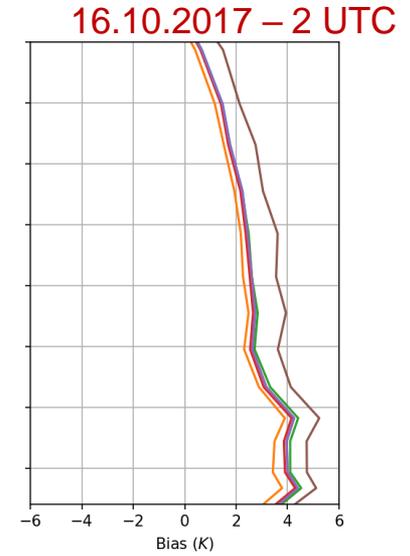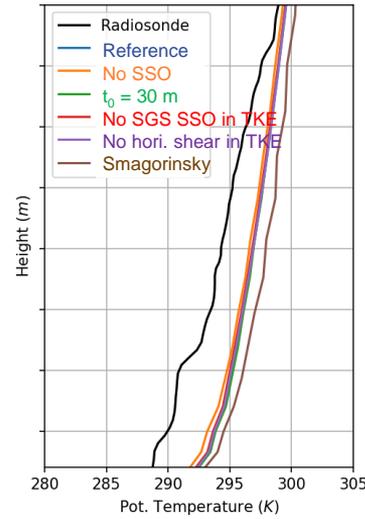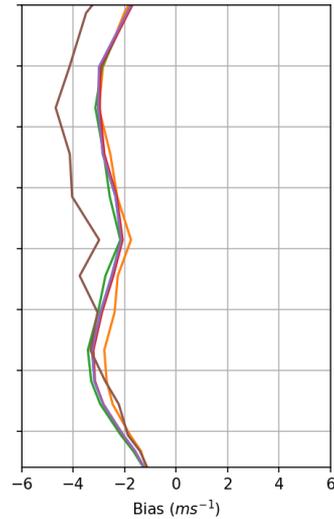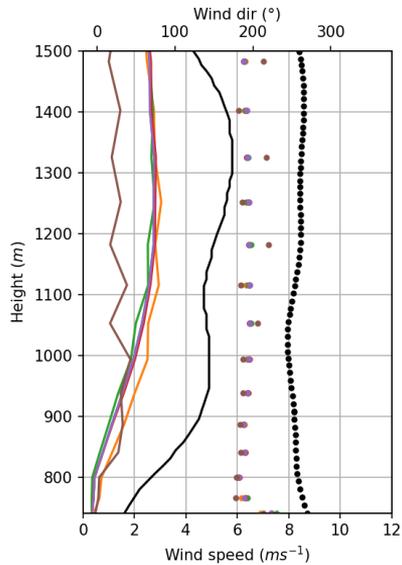
- Profiles do not change much by changing TKE (for example from hor. shear to $t_0 = 30m$).
- SSO seems more relevant.
- First experiments with Smagorinsky → too few turbulence near the surface?

Fluxes in Case Study
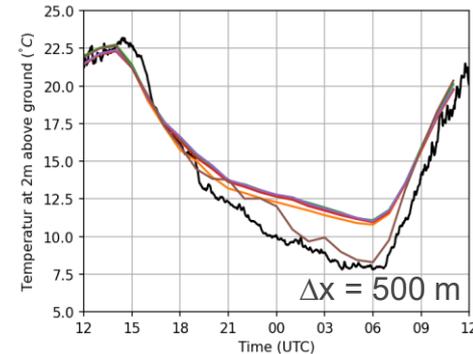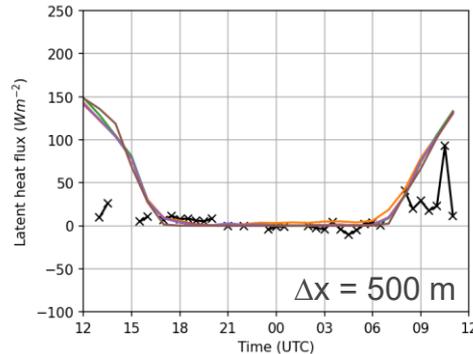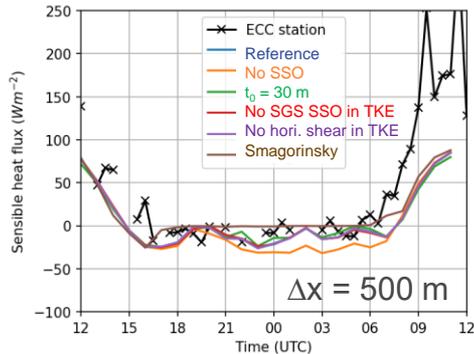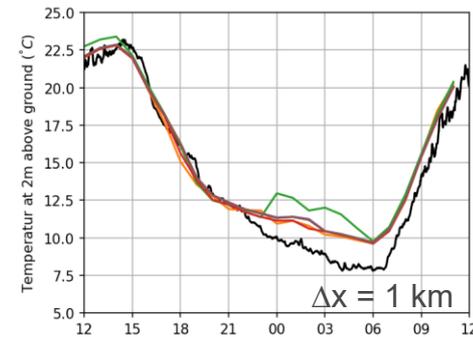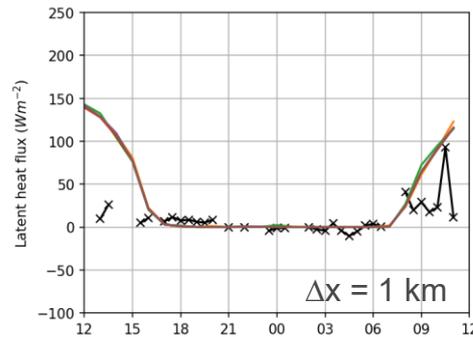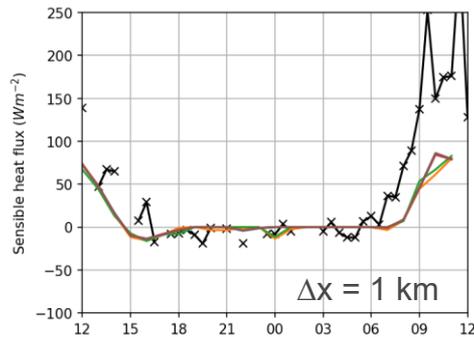
- Larger surface sensible heat flux and related 2 m temperature.
- Smagorinsky seems to be in good agreement with the observation with increasing resolution.

Conclusion & Outlook

- The model performance improves with increasing horizontal grid scale from 2 km and 1 km, mainly in valleys. Not necessarily for 500 m.

- Shallow-convection seems to get resolved starting with very high horizontal grid scales of 500 m. Switching off convection improves the scores for the valleys.

- However, increasing the horizontal grid scales does not lead to better weather forecast.

- Parameterized turbulence does not have a big influence on the results. Changes in the TKE scheme seem neglectable. Too much emitted heat during night time.

- Next:
    - Verification with Smagorinsky
    - Investigation of (scale depending) clouds and precipitation.
    - FESSTVaL Case Study (with different LATBC)

GLORI Partners and HPC system

Appendix
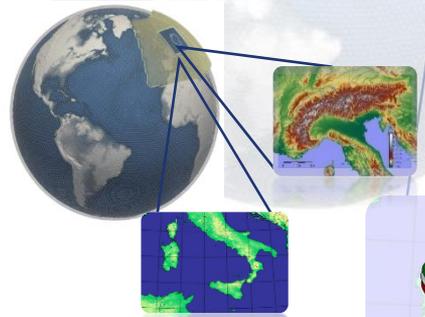
A. Plateau Stations

B. Model Setup

C. Case Study CAP 2017

D. Turbulence Scheme

E. Error Calculation

References:

Presentation   Model Physics

Radiation in Case Study

Δx = 1 km
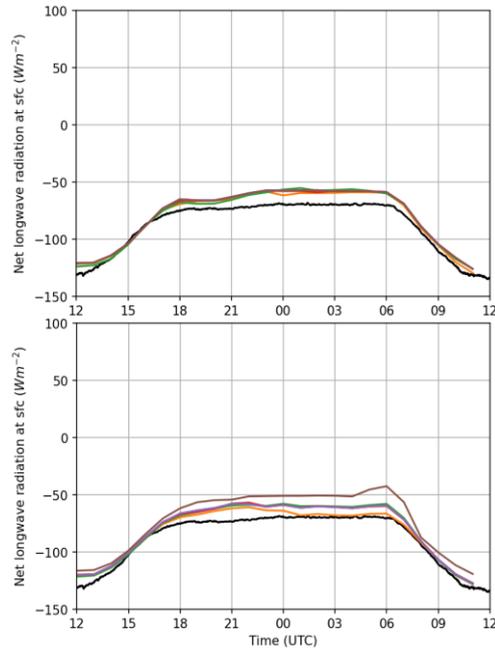
Δx = 500 m
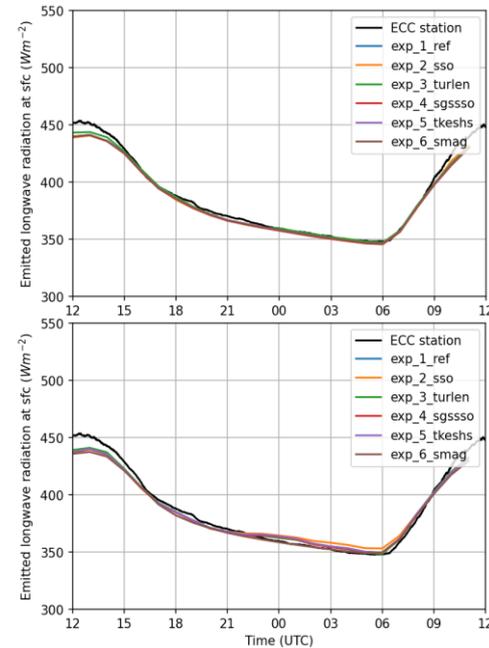
- Downwarded longwave radiation seems to be underestimated → issue in the LATBC?

A. Plateau Stations
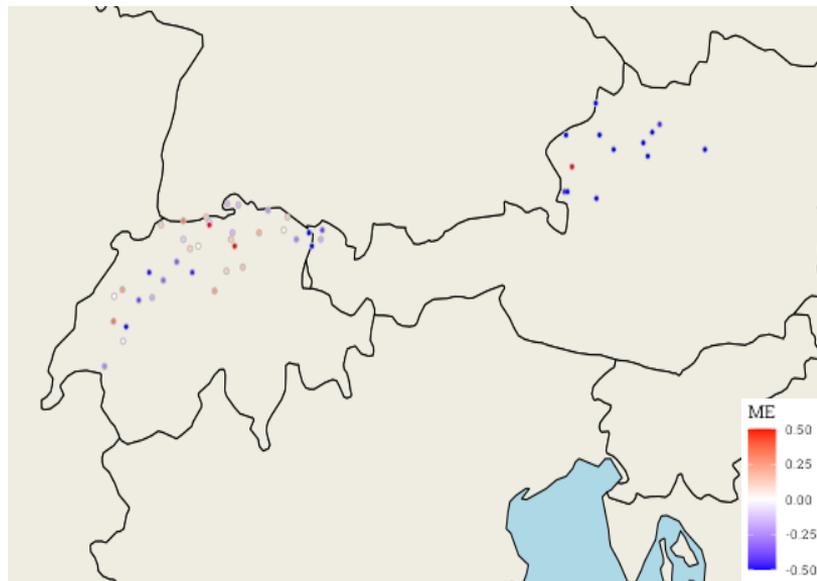
Station	Wind speed	Temperature
Plateau	51	50

Figure: The Plateau stations used for the comparison to the model results. The colors show the mean error (ME) of the model for the temperature at 2m height above ground.

GL⬤RI
GLObal to Regional ICON Digital Twin

RMSE (top) and ME (below) for June 2024

Initial hour: 12 h
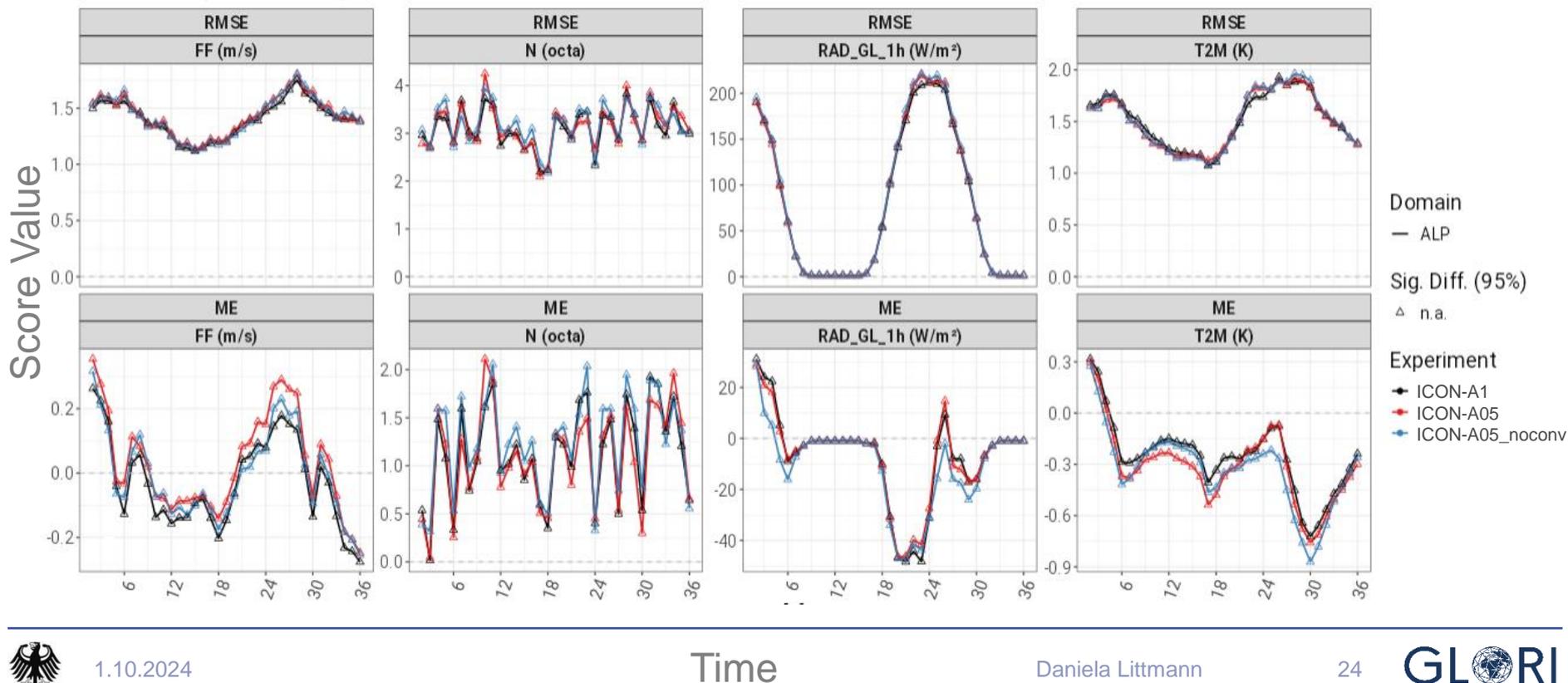
B. ICOsahedral Non-hydrostatic Model
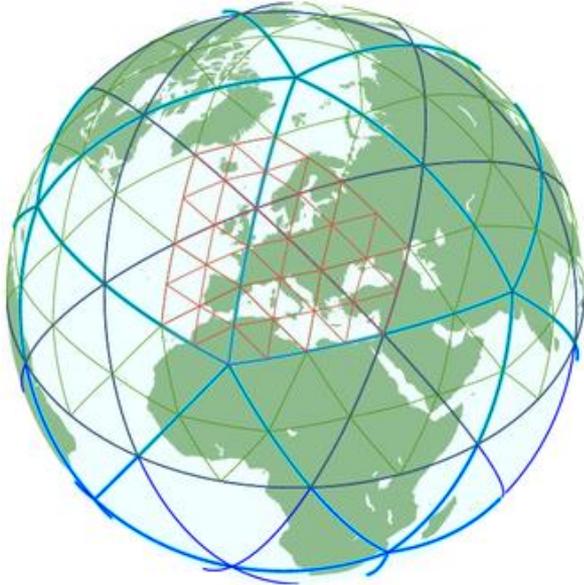
Prill et al. (2020)

- Fully compressible non-hydrostatic core

- Unified model system (climate & numerical weather prediction)

- From low resolution (~80 km) to high-resolution (~75 m)

- Triangular grid → No pole problem

GL⊕RI
GLObal to Regional ICON Digital Twin

B. Model Setup of ICON-LAM*

Physics Configuration

Orography	Orographic gravity wave drag
Mircrophysics	Double-moment
Turbulence	Turbdiff (TKE closure)
Sfc Transfer	Turbtran (TKE extension)
Convection	Shallow convection
Land Surface	TERRA

1. *Lott and Miller (1997)*
2. *Seifert and Beheng (2006)*
3. *Mellor and Yamada (1982), and Raschendorfer (2001)*
4. *Tiedke (1989), and Bechthold et al. (2008)*
5. *Schrodin and Heise (2001), Schulz et al. (2016)*

Model top	22 km
Vertical level	65 full (66 half)
Hor. grid scale	2 km, 1 km, 500 m, 250m
LATBC (at start)	Forecast (ICON-EU)
Forecast restart	12 h
Duration	36 h
1-way-Nesting	
Model version icon-2024.07	

* Limited Area Mode

B. Adapted gust parameterisation (AGP)

- New gust diagnostic option for large eddy permitting model applications

- AGP uses 10 min averaged 10 m wind speeds as input

- Scale dependent boundary layer constraint to avoid unrealistic wind speed maxima at the top of mountains
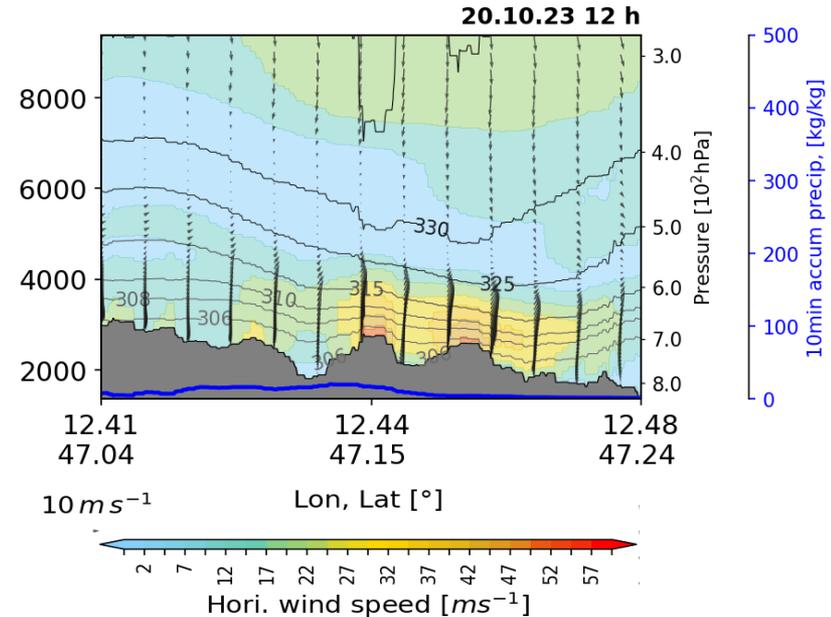
C. Model Domain for CAP 2017

Surface above sea level [m]

Δx

2 km

1 km

500 m

250 m
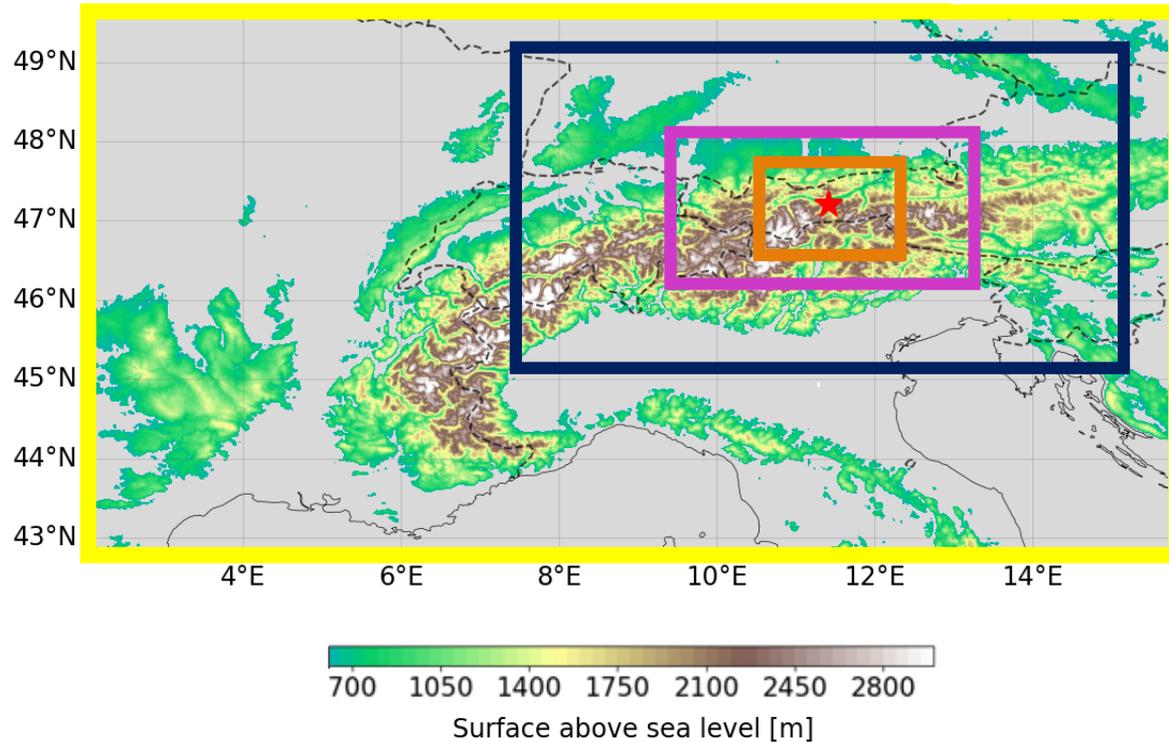
★ Station site

C. PIANO Observation

<u>**P**enetration and **I**nterruption of **A**lpi**N**e F**O**ehn (2017)</u>

- Inn Valley and Wipp Valley
- Fall & early winter
- Study erosion and cold air pools

MOMAA weather station data M0*
Radiosonde data INN
Flux station data EC*

Gohm et al. 2021
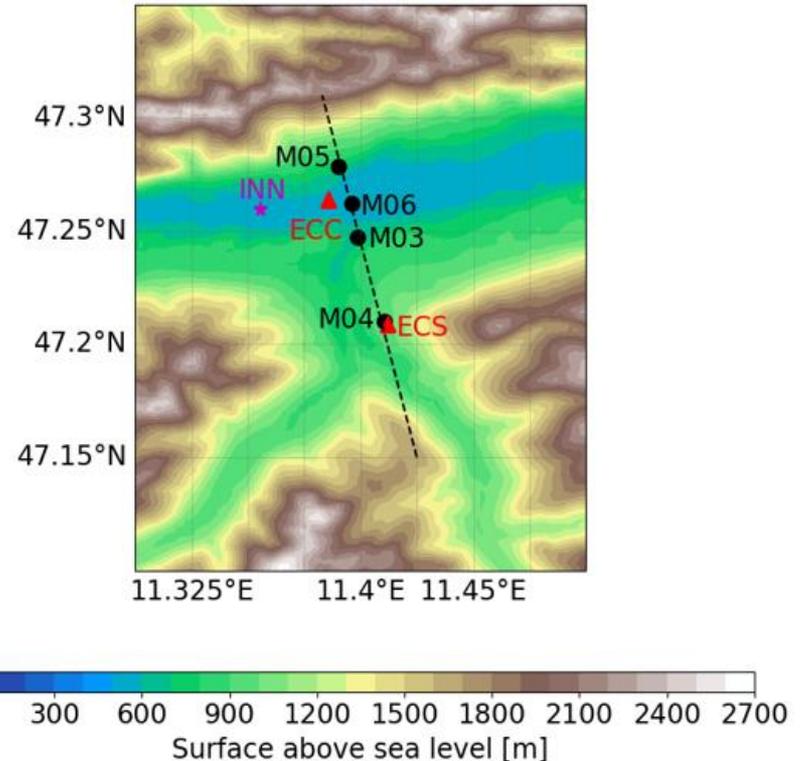
D. Turbulence Scheme: Turbdiff

Turbulent kinetic energy equation:

$$\frac{d}{dt}\frac{q^2}{2} = -K_h\frac{g}{\theta}\frac{\partial\hat{\theta}}{\partial z} + K_m\left[\left(\frac{\partial\hat{v}_i}{\partial z}\right)^2 + \left(\frac{\partial\hat{v}_j}{\partial z}\right)^2\right] + \frac{1}{\bar{\rho}}\frac{\partial}{\partial z}\left[\alpha\bar{\rho}lq\frac{\partial}{\partial z}\left(\frac{q^2}{2}\right)\right] - \frac{q^3}{B_1 l}$$

Buoyancy   Vertical shear production   Vertical turbulent transport   Dissipation

Turbulent velocity scale:

$$q = \sqrt{2e}$$

Turbulent diffusion coefficients:

$$K_m = lS_m q$$

$$K_h = lS_h q$$

Master length scale:

$$l = \frac{\kappa z}{1 + \frac{\kappa z}{l_0}}$$

Blackadar (1962)

S_m Stability function for momentum after Mellor-Yamada,
S_h Stability function for scalars after Mellor-Yamada,
θ Potential temperature,
$\hat{v}_i, \hat{v}_j$ Mean Horizontal Wind speed component,
$\bar{\rho}$ Density of air,
α Tunable parameter,
$B_1 = 16.6$ Model constant after Mellor-Yamada,
g Gravitaional acceleration,
$l_0 = 300\,\text{m}$ Asymptotic length scale,
$\kappa = 0.4$ von Karman constant

GL🌐RI
GLObal to Regional ICON Digital Twin

TKE

K_M, K_H, q

z1

T, QV, U, V

Lowest atmospheric main level

Surface layer

r_{sfc}

K_{M0}, K_{H0}, q_0

z0

Roughness layer

r_{rgn}

Transfer layer

0
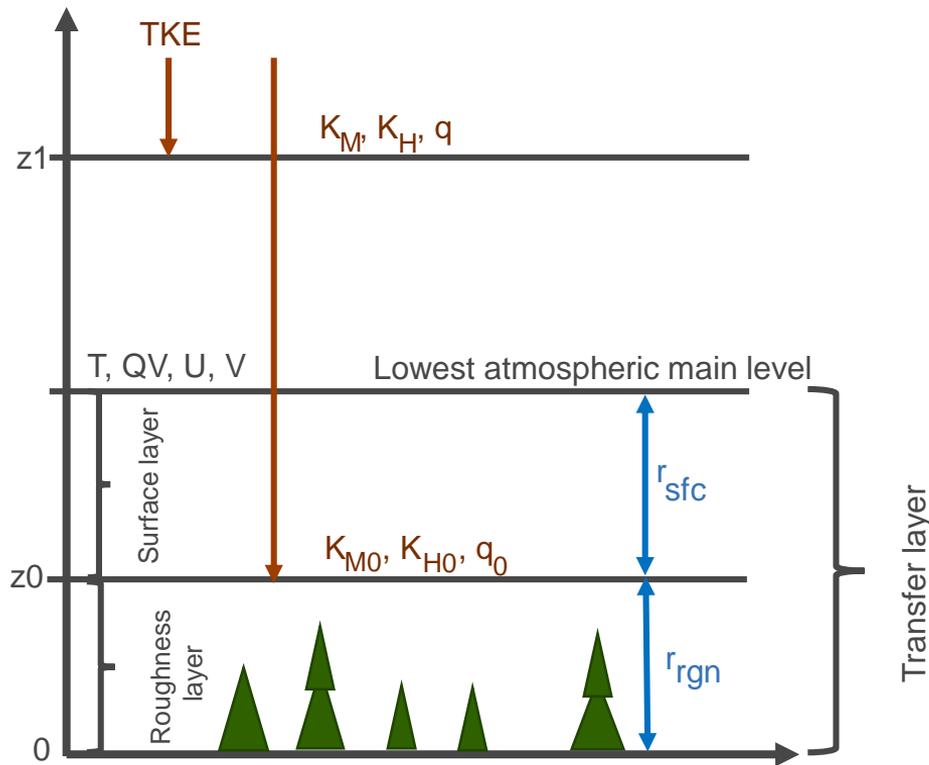
The turbulence scheme is applied to the top of the lowermost atm. layer and the top roughness layer

→ The transfer coefficients are expressed as functions of the **turbulent diffusion coefficients** and the sum of the **resistance terms**

→ The final fluxes are determined by a **drag formulation**

Raschendorfer (2001)

D. Turbulence Scheme: 3D-Smag

Turbulent parametrization term:

$$Q(v_i) = \left(\frac{\partial \hat{v}_i}{\partial t}\right)_{turb} = \frac{1}{\bar{\rho}} \frac{\partial \tau_{ij}}{\partial x_k}$$

Stress tensor:

$$\tau_{ij} = K_m \left(\hat{S}_{ij} - \frac{1}{3}\hat{S}_{kk}\delta_{ij}\right)$$

Eddy exchange coefficients:

$$K_m = K_h Pr_t$$

$$K_h = \begin{cases} 2l_s\bar{\rho}|S|\sqrt{1 - \frac{R_i}{Pr_t}} & , 1 - \frac{R_i}{Pr_t} > 0 \\ 0.001 \text{ m}^2\text{s}^{-1} & , 1 - \frac{R_i}{Pr_t} \leq 0 \end{cases}$$

Subgrid length scale:

$$l_s = \frac{(c_s \Delta)^2}{1 + \left(\frac{c_s \Delta}{\kappa z_g}\right)^2}$$

Favre-averaged rate of strain tensor:

$$\hat{S}_{ij} = \frac{1}{2}\left(\frac{\partial \hat{v}_i}{\partial x_j} + \frac{\partial \hat{v}_j}{\partial x_i}\right)$$

K_m Eddy exchange coefficient for momentum,
K_θ Eddy exchange coefficient for heat,
$\hat{S}_{ij}$ Strain rate tensor,
Δ Grid volume,
l_s Subgrid length scale,
z_g Geopotential height,
$c_s = 0.23$ Smagorinsky constant,
R_i Richardson number,
$Pr_t = 0.7$ Prandtl number,
$\kappa = 0.4$ von Karman constant

Lilly (1962)

Smagorinsky (1963)

Dipankar (2015)

D. Turbulence Scheme: Bulk-Transfer

Surface fluxes flux:

$$Q_{m_{i,j}} = -\bar{\rho} C_d |\hat{v}| \hat{v}_{i,j}$$

$$Q_s = -\bar{\rho} C_h |\hat{v}| \left(c_p(\hat{\theta}_1 - \hat{\theta}_{sfc}) + \Phi\right)$$

$$Q_l = -\bar{\rho} C_h |\hat{v}| (\hat{q}_{v\_1} - \hat{q}_{v\_sfc}) L \qquad , L = \begin{cases} L_s, & H_i > 0 \\ L_v, & H_i = 0 \end{cases}$$

Dimensionless transfer coefficiens:

$$C_d = C_{dn} f_m(R_i)$$

$$C_h = C_{hn} f_h(R_i)$$

Horizontal wind speed at the lowest model level:

$$|\hat{v}| = \sqrt{\hat{v}_i^2 + \hat{v}_j^2}$$

Q_s Sensible heat flux at surface,

Q_l Latent heat flux at surface,

$Q_{mi,j}$ Momentum flux at surface,

C_d Dimless. transfer coeff. for momentum,

C_h Dimless. transfer coeff. for scalars,

C_{dn} Neutral transfer coeff. for momentum,

C_{hn} Neutral transfer coeff. for scalars,

f_m Stability function for momentum,

f_h Stability function for heat,

$\bar{\rho}$ Density of air of lowest atm. layer,

Φ Geopot. Thickness,

L_s Latent heat of sublimation,

L_v Latent heat of vaporization

Dyer-Businger (1971) & Louis (1979)

Deutscher Wetterdienst
Wetter und Klima aus einer Hand

Mean Error, Bias:
(Square unit of variable)

$$ME = \frac{1}{n} \sum_{i=1}^{n} |y_i - x_i|$$

Root Mean Square Error:
(Same unit as variable)

$$RMSE = \sqrt{\frac{1}{n} \sum_{i=1}^{n} (y_i - x_i)^2}$$

y : Prediction

x : Observation

n : Sample size